



โครงการ

การเรียนการสอนเพื่อเสริมประสบการณ์

ชื่อโครงการ การศึกษาโครงสร้างของซีโอไลติกอิมิดาโซเลตเฟรมเวิร์ก-8 และการกักเก็บแก๊สมีเทนโดยวิธีดีเอฟทีบี

A study of ZIF-8 structure and its methane storage by DFTB method

ชื่อนิสิต นายนนธวัช พลอยสงศรี

ภาควิชา เคมี

ปีการศึกษา 2559

คณะวิทยาศาสตร์ จุฬาลงกรณ์มหาวิทยาลัย

A study of ZIF-8 structure and its methane storage by DFTB method
การศึกษาโครงสร้างของซีโอไลติกอิมิดาโซเลตเฟรมเวิร์ก-8 และการกักเก็บแก๊สมีเทนโดยวิธีดีเอฟทีบี

Mr. Nontawat Ploysongsri

Submitted to the Department of Chemistry Chulalongkorn University
in partial fulfillment of the requirements for the Bachelor's degree in Chemistry
Department of Chemistry Faculty of Science Chulalongkorn University
Academic Year 2016

Project Title: A study of ZIF-8 structure and its methane storage by DFTB method


Student name: Mr. Nontawat Ploysongsri

Field of study: Chemistry

Project Advisor: Professor Vithaya Ruangpornvisuti, Dr.rer.nat.

Accepted by Department of Chemistry, Faculty of Science, Chulalongkorn University in Partial Fulfillment of the Requirements for the Degree of Bachelor of Science.

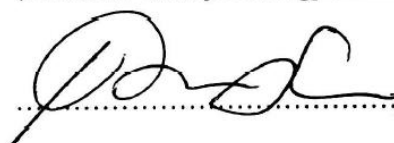
PROJECT COMMITTEE

.....Chairman

(Associate Professor Buncha Pulpoka, Ph.D.)

.....Project Advisor

(Professor Vithaya Ruangpornvisuti, Dr.rer.nat.)

.....Examiner

(Associate Professor Pornthep Sompornpisut, Ph.D.)

This report has been endorsed by Head of Department of Chemistry

.....Head of Department of Chemistry

(Associate Professor Vudhichai Parasuk, Ph.D.)

..... May 2017

Writing quality of this report is: Very good Good Pass

Project Title A study of ZIF-8 structure and its methane storage by DFTB method

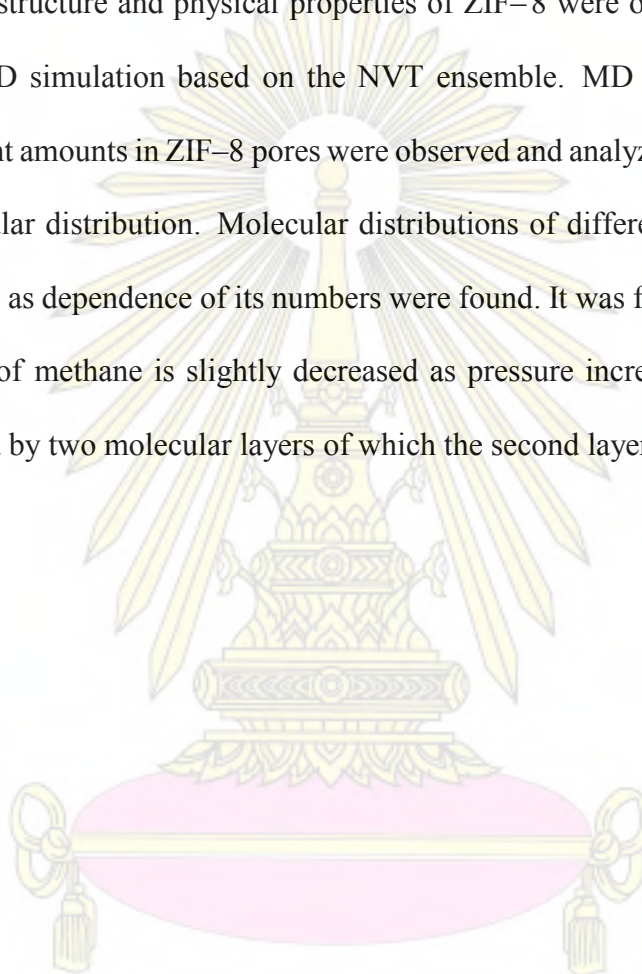
Student name Mr. Nontawar Ploysongsri Student ID 5633089323

Advisor name Professor Vithaya Ruangpornvisuti, Dr.rer.nat.

Department of Chemistry, Faculty of Science, Chulalongkorn University, Academic Year 2016

Abstract

The electronic structure and physical properties of ZIF-8 were obtained using the SCC-DFTB method and MD simulation based on the NVT ensemble. MD simulations of methane molecules with different amounts in ZIF-8 pores were observed and analyzed in terms of diffusion, adsorption and molecular distribution. Molecular distributions of different numbers of methane molecules in the ZIF-8 as dependence of its numbers were found. It was found that inter distances between carbon atom of methane is slightly decreased as pressure increased and each methane molecule was surround by two molecular layers of which the second layer contains larger number than the first.



Keywords: ZIF-8, methane diffusion, radial distribution of C-C atoms, DFTB, SSC-DFTB

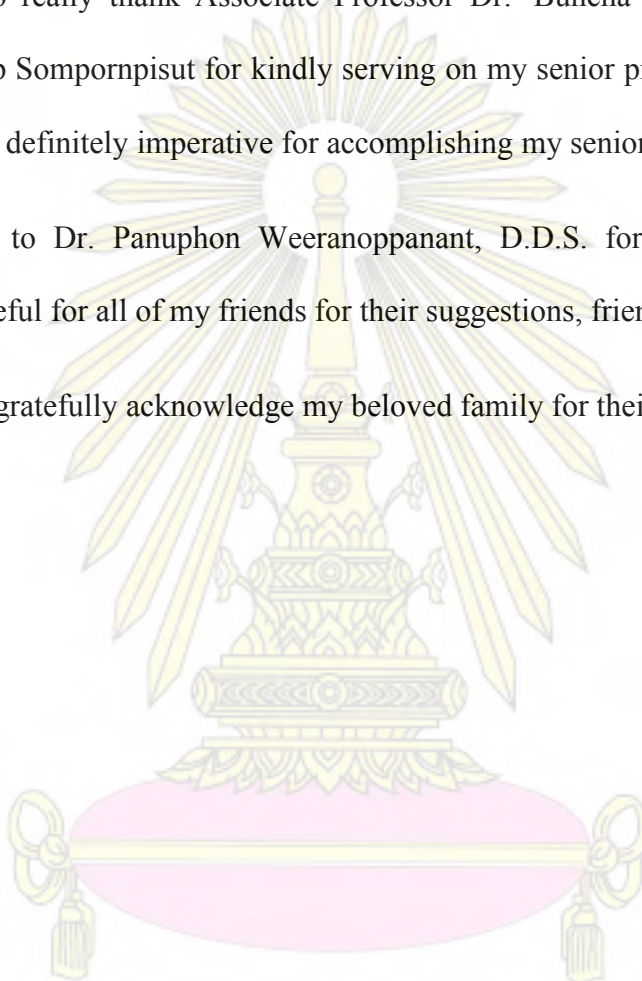
ACKNOWLEDGEMENTS

I would like to express my sincere thanks to advisor Professor Dr. Vithaya Ruangpornvisuti for his very useful guidance, understanding and constant support throughout the course of this research.

I would like to really thank Associate Professor Dr. Buncha Pulpoka and Associate Professor Dr. Pornthep Sompornpisut for kindly serving on my senior project committee. Their sincere suggestions are definitely imperative for accomplishing my senior project.

Special thanks to Dr. Panuphon Weeranoppanant, D.D.S. for being my inspiration. Furthermore, I am grateful for all of my friends for their suggestions, friendship and all their help.

Finally, I most gratefully acknowledge my beloved family for their always supporting me.



CONTENTS

	Page
ABSTRACT IN THAI.....	III
ABSTRACT IN ENGLISH.....	IV
ACKNOWLEDGEMENTS.....	V
CONTENTS.....	VI
LIST OF FIGURES.....	IX
LIST OF TABLES.....	X
CHAPTER I INTRODUCTION.....	1
1.1 Background and Literature review.....	1
1.2 Theoretical background.....	3
1.2.1 Ab initio method.....	3
1.2.2 Density functional theory (DFT) method.....	4
1.2.2.1 Kohn-Sham equations.....	5
1.2.3 Density-functional tight-binding (DFTB) method.....	7
1.2.3.1 DFTB1.....	7
1.2.3.2 DFTB2.....	9
1.2.3.3 DFTB3.....	9
1.2.4 Molecular dynamics (MD) simulation.....	10
1.2.4.1 Canonical (NVT) ensemble.....	10

	Page
1.2.4.2 Andersen thermostat.....	10
1.2.4.3 Berendsen thermostat.....	10
1.3 Objective.....	11
CHAPTER II COMPUTATIONAL DETAILS.....	12
2.1 Molecular dynamics simulation.....	12
2.2 Definition of reaction terms.....	12
2.2.1 Diffusion of small gas in ZIF-8.....	12
2.2.1.1 The mean-square displacement (MSD).....	12
2.2.1.2 The self-diffusion coefficient.....	13
2.2.1.3 The radial distribution function (RDF).....	13
2.2.2 Adsorption of small gases in ZIF-8.....	14
CHAPTER III RESULTS AND DISCUSSIONS	
3.1 Geometry optimization of ZIF-8.....	15
3.2 Energies of various structures of ZIF-8 pore.....	18
3.3 MD simulations and dynamical quantities of CH ₄ in ZIF-8 pore.....	21
CHAPTER IV CONCLUSIONS.....	30

	Page
REFERENCES.....	31
VITAE.....	35

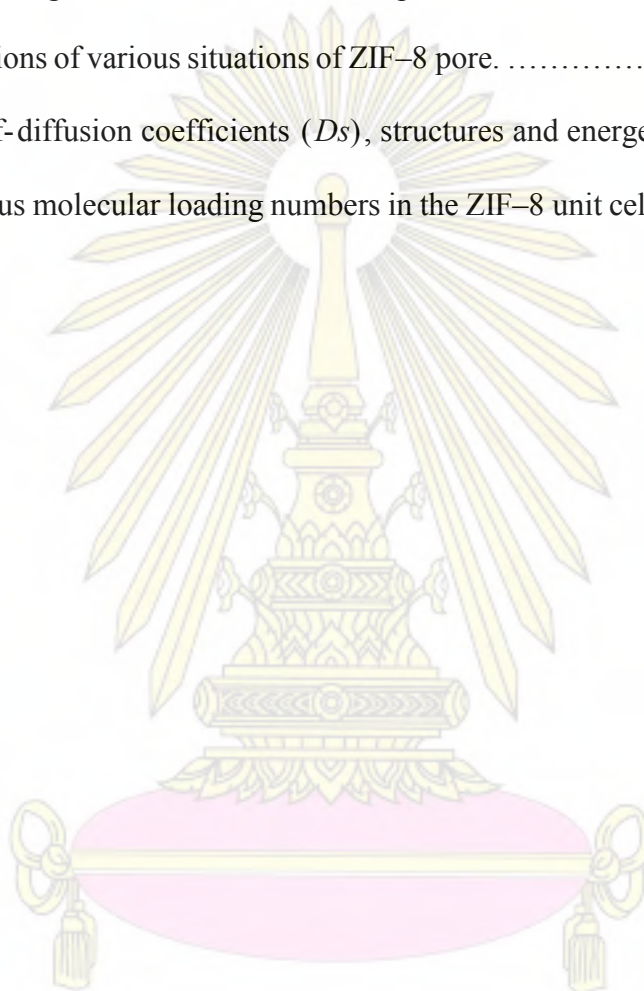


LIST OF FIGURES

Figure		Page
3.1	The SCC–DFTB optimized unit cell–sized ZIF–8 structure (a) with and (b) without electrostatic surfaces.....	15
3.2	Plot of total energy (au) of the ZIF–8 against lattice parameter a including its quadratic function ($E_{\text{total}} = 0.18857a^2 - 6.30013a - 326.64929$). The minimum value derived by equation $dE_{\text{total}}/da = 0$, $a = 16.7050 \text{ \AA}$ was obtained.	16
3.3	Labeling atoms of ZIF–8 for as referred in Table 3.1.	18
3.4	MD simulations based on (a) Andersen and (b) Berendsen thermostats, NVT ensemble presented as energies (left) and temperature (right) fluctuations of ZIF–8 with unit cell–sized structure.	20
3.5	The center–of–mass radial density profile of CH ₄ from the center of the ZIF–8 unit–cell pour for the systems containing (a) 8, (b) 12 and (c) 16 CH ₄ molecules.	25
3.6	The C–C radial distribution function of CH ₄ molecules in the systems of (a) 8, (b) 12 and 16 CH ₄ molecules in the ZIF–8 unit cell.	26
3.7	The final snapshot of the simulation box involves the distribution of methane 16 molecules.	27
3.8	The C–C radial distribution function of CH ₄ molecules in terms of $n(r)$ (left axis) and $N(r)$ (right axis) of (a) 8, (b) 12 and 16 CH ₄ molecules in the ZIF–8 unit cell.	28
3.9	Plot of D_s against the number (N) of methane molecules in the ZIF–8 unit cell. The dot line is the quadratic fitted curve $D_s = -4.375 \times 10^{-12} N^2 + 1.65 \times 10^{-10} N + 5.70 \times 10^{-10}$	29

LIST OF TABLES

Table		Page
3.1	Selected geometrical parameters of ZIF-8, based on X-ray diffraction and DFTB optimized structures.	17
3.2	Total energies of SCC- DFTB- optimized structure and MD simulations of various situations of ZIF-8 pore.	19
3.3	The self-diffusion coefficients (D_s), structures and energetics of CH ₄ in various molecular loading numbers in the ZIF-8 unit cell, at 298 K..	24



CHAPTER I

INTRODUCTION

1.1 Background and Literature review

Zeolitic Imidazolate Frameworks (ZIFs) are a subclass of the metal-organic frameworks (MOFs) which were formed by metal i.e. Zn, Cu, and Co linked with imidazolate group in tetrahedral geometry. ZIF-8 one of the ZIFs has the sodalite topology and has large pores and small pores (11.6 and 3.4 Å, respectively)¹. Furthermore, ZIF-8 has high thermal and chemical stability¹, high flexibility²⁻³ and permanent porosity⁴. Thus it has been applied in different kinds such as gas diffusion, separation and storage, etc.⁵⁻⁶ Pimental and Lively⁵ studied on the separation of light hydrocarbons, ethane, propane, propylene and butane by ZIF-8. In propane/butane mixtures, diffusive selectivity is not enough to separate two gases. For ethane/propane mixtures, the separation factor at 273 K is more than at 293 K because of the differences in the activation energies of permeation and heats of sorption make the kinetic selectivity is higher at the lower temperature. Furthermore, propane/propylene mixtures are separated because the different value of diffusive selectivity. Lai *et al.*⁷ studied on the separation of CO₂ from CH₄ via ZIF-8 membrane. The result showed that the highest CO₂/CH₄ separation factor was observed at low CO₂ composition and adsorptions between CO₂ and CH₄ are competitive adsorption. CH₄ is one of the natural gas components, which can be used as a fuel⁸. Therefore, it is necessary for storage of CH₄ in order to reduce it from the atmosphere and consume it in the industry. ZIF-8 is the one of CH₄ adsorbent candidates. In the recent years, many researchers investigate CH₄ adsorption, diffusion, separation and storage ability of ZIF-8⁹⁻¹⁰. Eyer *et al.*¹¹ studied the adsorption of CH₄/N₂ on ZIF-

8 and other commercial adsorbents. The results showed that ZIF-8 has good selective properties and high surface area, but ZIF-8 has weak binding interaction with CH₄. Thus, ZIF-8 has lower adsorption capacity than Hayasap D, another commercial adsorbent, in the low pressure and high temperature regime. Krokidas *et al.*¹⁰ used new structure force-field parameters for molecular dynamics (MD) simulation to study the diffusion of CH₄ in ZIF-8. The transport diffusivities of CH₄ from MD simulation are similar to the transport diffusivities from infrared microscopy and more accuracy than the value from literature MD simulations. Alirezaie *et al.*¹² studied the diffusion of O₂, N₂ and CH₄ in polyethylene and polyethylene/ montmorillonite- clay nanocomposite films with different silicate layers configurations by molecular dynamics simulation within NVT ensemble. They found that the diffusion coefficient of O₂ is higher than N₂ and CH₄. Kadoura *et al.*¹³ used molecular dynamics simulations to study the transport properties of CO₂, CH₄ and CO₂/CH₄ mixtures in Na-montmorillonite clay. The simulation showed that the self-diffusion coefficient of pure CO₂ and CH₄ decreased when their loading increased. The diffusion of CO₂ was not obviously affected by CH₄ for CO₂/CH₄ mixture compositions. They attributed this to the preferential adsorption of CO₂ over CH₄. Fairen-Jimenez *et al.*¹⁴ studied flexibility and swing effect on the adsorption of CO₂, CH₄ and alkanes on ZIF-8 by gas adsorption experiments and Grand canonical Monte Carlo (GCMC) simulations. They compared UFF, UFF (+), for which only Lenard-Jones parameter ϵ was adjusted, and UFF (*), for both Lenard-Jones parameter, ϵ and σ , were adjusted force field, they found that UFF (+) was accurately predicted the experimental results. They found that the most favorable CH₄ adsorption site is the C=C double bond of imidazolate group. Finally, they concluded that the change of ZIF-8 structure arising with increase in the number of adsorbed CH₄ molecules.

Density-functional tight-binding (DFTB)¹⁵ is the method that based on density-functional theory (DFT). The advantage of DFTB is that DFTB can calculate in the larger system than DFT because DFT has system sizes limits. Next, DFTB can access longer time scales than DFT. DFTB can be employed on dynamical properties. Garberoglio and Tioli¹⁶ studied the flexibility of ZIF-8 and the diffusion barrier for H₂, CO₂ and CH₄ by DFTB method comparison with the Universal force field (UFF). The results indicated that DFTB is more accuracy than UFF.

In the present work, the physical properties of ZIF-8 and diffusion of CH₄ in ZIF-8 were studied using MD/DFTB method.

1.2 Theoretical background

Quantum chemical calculation has been used to calculate structures, properties and interaction of molecules¹⁷. Density-functional tight-binding (DFTB), one of quantum mechanics method based on density functional theory was employed to calculate in the present work.

1.2.1 Ab initio method

Ab initio calculation methods¹⁸ are method of computational chemistry based on quantum mechanics. This method associates with Schrödinger equation as shown in equation (1.1).

$$-\frac{\hbar^2}{2m}\nabla^2\Psi(r,t)+V(r)\Psi(r,t)=i\hbar\frac{\partial\Psi(r,t)}{\partial t} \quad (1.1)$$

where $\hbar = \frac{h}{2\pi}$ and h is Planck's constant, m is particle's mass. ∇^2 is the Laplacian's operator

which is given by $\nabla^2 = \frac{\partial^2}{\partial x^2} + \frac{\partial^2}{\partial y^2} + \frac{\partial^2}{\partial z^2}$ in Cartesian coordinates. $V(r)$ is the potential energy

function and $\Psi(r,t)$ is a time-dependent wave function.

This equation needs the same time and position independent constants to resolve. The constant could be energy of the particle, the left-hand side of the equation is thus set equal to the constant. After the modification of equation (1.1), yields in equation (1.2).

$$-\frac{\hbar^2}{2m}\nabla^2\Psi(r)+V(r)\Psi(r)=E\Psi(r) \quad (1.2)$$

This equation is called the time-independent Schrödinger equation, which depends only on position. The left-hand side is the operator called the Hamiltonian, \hat{H} such that.

$$\hat{H}\Psi(r)=E\Psi(r) \quad (1.3)$$

where

$$\hat{H}=-\frac{\hbar^2}{2m}\nabla^2+V(r) \quad (1.4)$$

An operator is easily transformed from one function to another function. All measurable value such as energy, momentum etc. are set as operators.

$$\hat{H}\Psi(r)=E\Psi(r) \quad (1.5)$$

1.2.2 Density functional theory (DFT) method

Density functional theory (DFT) methods are constructed by The Hohenberg-Kohn (HK) theorems¹⁹. The HK theorems make the electronic density as variable to electronic-structure calculations and the energy of a molecule is obtained from the electron density instead of a wave function.

1.2.2.1 Kohn-Sham equations

Kohn and Sham method was used to solve the problem of interacting electrons onto a fictitious system of non-interacting electrons²⁰. The solution starts from using mono-electronic orbitals to calculate the kinetic energy. In a system of N non-interacting electrons and the external potential v_s , with Hamiltonian.

$$\hat{H}_s = \sum_i^N \frac{1}{2} \nabla_i^2 + \sum_i^N v_s(\vec{r}_i) = \sum_i^N \hat{h}_s \quad (1.6)$$

where

$$\hat{h}_s = -\frac{1}{2} \nabla_i^2 + v_s(\vec{r}_i) \quad (1.7)$$

In which there are no electron repulsion terms and electronic density is exactly the same as in the system of interacting electrons. All electronic densities for the system of the single particle orbitals $\psi_i(\vec{r})$ can be written as

$$\rho(\vec{r}) = \sum_i^N |\psi_i(\vec{r})|^2 \quad (1.8)$$

Thus, the Hohenberg-Kohn functional can be written in the form

$$F_{HK}[\rho] = T_s[\rho] + J[\rho] + E_{xc}[\rho] \quad (1.9)$$

where T_s represents the kinetic-energy functional, given by

$$T_s[\rho] = \sum_i^N \left\langle \psi_i \left| -\frac{1}{2} \nabla_i^2 \right| \psi_i \right\rangle \quad (1.10)$$

J represents the classic Coulomb interaction functional

$$J[\rho] = \frac{1}{2} \iint \frac{\rho(\vec{r})\rho(\vec{r}')}{|\vec{r} - \vec{r}'|} d\vec{r} d\vec{r}' \quad (1.11)$$

E_{xc} is the exchange-correlation functional, which is defined by the difference between the exact kinetic energy T and T_s and the difference between the non-classic part of the Coulomb interaction (V_{ee}) and the classic Coulomb interaction.

$$E_{xc}[\rho] = T[\rho] - T_s[\rho] + V_{ee}[\rho] - J[\rho] \quad (1.12)$$

Then, the chemical potential can be written as

$$\mu = v_{KS}(\vec{r}) + \frac{\delta T_s[\rho]}{\delta \rho(\vec{r})} \quad (1.13)$$

where v_{KS} is the Kohn-Sham (KS) effective potential, which is defined as

$$\begin{aligned} v_{KS}(\vec{r}) &= v_{ext}(\vec{r}) + \frac{\delta J[\rho]}{\delta \rho(\vec{r})} + \frac{\delta E_{xc}[\rho]}{\delta \rho(\vec{r})} \\ &= v_{ext}(\vec{r}) + \int \frac{\rho(\vec{r}')}{|\vec{r} - \vec{r}'|} d\vec{r}' + v_{xc}(\vec{r}) \end{aligned} \quad (1.14)$$

where v_{ext} is the external potential and the exchange-correlation potential v_{xc} is defined as

$$v_{xc}(\vec{r}) = \frac{\delta E_{xc}[\rho]}{\delta \rho(\vec{r})} \quad (1.15)$$

Equation (1.13), restricted by $\int \rho(\vec{r}) d\vec{r} = N$, is the same equation that would be received for a system of N non-interacting electrons submitted to the external potential $v_{KS} = v_S$. Thus, for taken v_{KS} a suitable value of ρ can be calculated for equation (1.13) by solving the N mono-electronic equations.

$$\left[-\frac{1}{2}\nabla^2 + v_{KS}(\vec{r}) \right] \psi_i = \varepsilon_i \psi_i \quad (1.16)$$

The total energy can be calculated by the following expression.

$$E[\rho] = \sum_i^N n_i \left\langle \psi_i \left| -\frac{1}{2}\nabla^2 + v_{ext}(\vec{r}) + \frac{1}{2} \int \frac{\rho(\vec{r}')}{|\vec{r} - \vec{r}'|} d\vec{r}' \right| \psi_i \right\rangle + E_{xc}[\rho] + \frac{1}{2} \sum_{\beta}^N \sum_{\alpha \neq \beta}^N \frac{Z_{\alpha} Z_{\beta}}{|\vec{R}_{\alpha} - \vec{R}_{\beta}|} \quad (1.17)$$

1.2.3 Density-functional tight-binding (DFTB) method

DFTB can be derived from a Taylor expansion of the KS density functional total energy around a properly chosen reference density $\rho(r)^{19}$. A reference density $\rho^0(r)$ is perturbed by density fluctuation.

$$\rho(r) = \rho^0(r) + \delta\rho(r) \quad (1.18)$$

The exchange-correlation energy functional is expanded in a Taylor series and the total energy can be written as

$$E^{DFTB3}[\rho^0 + \delta\rho] = E^0[\rho_0] + E^1[\rho_0, \delta\rho] + E^2[\rho_0, (\delta\rho)^2] + E^3[\rho_0, (\delta\rho)^3] \quad (1.19)$$

1.2.3.1 DFTB1

DFTB1 or non-self-consistent DFTB (non-SCC DFTB) is contributed only the two first terms of equation (1.19), $E^0[\rho_0]$ and $E^1[\rho_0, \delta\rho]$. DFTB1 is based on linear combination of atomic orbital (LCAO) ansatz of the KS orbitals.

$$\psi_i = \sum_{\mu} c_{i\mu} \phi_{\mu} \quad (1.20)$$

The atomic orbitals (AOs) are obtained from DFT calculations of the corresponding atoms.

$$|\phi_\mu\rangle = |\phi_\mu^a\rangle - \sum_{b \neq a} \sum_{\kappa} |\phi_\kappa^b\rangle \langle \phi_\kappa^b | \phi_\mu^a \rangle, \mu \in \{a\} \quad (1.21)$$

where $|\phi_\mu^a\rangle$ is the valence AO μ at atom a and $|\phi_\kappa^b\rangle$ is a core orbital at atom b , as obtained from the corresponding atomic calculations.

The atomic KS equations are usually solved applying an additional potential to the atomic KS equations.

$$\left[-\frac{1}{2} \nabla^2 + v^{eff}[\rho^{atom}] + \left(\frac{r}{r_0} \right)^2 \right] \phi_\mu = \varepsilon_\mu \phi_\mu \quad (1.22)$$

Then, with AO basis and initial density determined, the KS equation can be solved leading to the energy.

$$E^1 = \sum_i n_i \varepsilon_i \quad (1.23)$$

where n_i is an occupation number of KS orbital i .

This is the electronic energy of the DFTB method. To find the total energy, the E^0 has to be approximated. In DFTB, this term is approximated by a sum of pair potentials called repulsive energy term.

$$E^0[\rho_0] \approx E_{rep} = \frac{1}{2} \sum_{ab} V_{ab}^{rep} \quad (1.24)$$

The total energy for DFTB1 is defined as

$$E^{DFTB1} = \sum_i n_i \varepsilon_i + \frac{1}{2} \sum_{ab} V_{ab}^{rep} \quad (1.25)$$

1.2.3.2 DFTB2

DFTB2 approximates E^2 term in equation (1.19) further. The density fluctuations are written as a superposition of atomic contributions.

$$\delta\rho = \sum_a \delta\rho_a \quad (1.26)$$

The atomic-like density fluctuations are expanded in a multipole expansion, however, only keeping the monopole term.

$$\delta\rho_a = \Delta q_a F_{00}^a \gamma_{00} \quad (1.27)$$

By evaluated assuming an exponentially decaying charge density

$$\delta\rho_a \approx \Delta q_a \frac{\tau_a^3}{8\pi} e^{-\tau_a |r-R_0|} \quad (1.28)$$

E^2 in (1.19) is defined as

$$E^2(\tau_a, \tau_b, R_{ab}) = \frac{1}{2} \sum_{ab} \Delta q_a \Delta q_b \gamma_{ab}(\tau_a, \tau_b, R_{ab}) \quad (1.29)$$

The Hartree term therefore describes the interaction of the charge density fluctuations $\delta\rho_a$ and $\delta\rho_b$, which reduces to Coulomb interaction of partial charges Δq_a and Δq_b for large distances, i. e. γ_{ab} approaches $1/R_{ab}$ for large distances.

1.2.3.3 DFTB3

For E^3 , the same approximations are introduced as for E^2 . The third-order terms describe the change of the chemical hardness of an atom with its charge state, a new parameter is introduced, the chemical hardness derivative. A function Γ_{ab} results as derivative of the γ -function with respect to charge by introducing the Hubbard derivative parameter.

With all these approximations, the SCC-DFTB total energy in the third order is given by

$$E^{DFTB3} = \sum_{iab} \sum_{\mu \in a} \sum_{\nu \in b} n_i c_{\mu} c_{\nu} H_{\mu\nu}^0 + \frac{1}{2} \sum_{ab} \Delta q_a \Delta q_b \gamma_{ab}^h + \frac{1}{3} \sum_{ab} \Delta q_a^2 \Delta q_b \Gamma_{ab} + \frac{1}{2} \sum_{ab} V_{ab}^{rep} \quad (1.30)$$

1.2.4 Molecular dynamics (MD) simulation

Molecular dynamics (MD) simulations are useful method to study in physical chemistry. Because, the time evolution of chemical system and many phenomena such as chemical reactions, diffusion described by MD simulation. MD simulations can be calculated by molecular mechanics (MM), quantum mechanics (QM) and hybrid of QM and MM (QM/MM)²¹⁻²³.

1.2.4.1 Canonical (NVT) ensemble

In the canonical ensemble, the quantities of substance (N), volume (V) and temperature (T) are preserved. In NVT ensemble, the energies of endothermic and exothermic processes are exchanged with a thermostat²⁴.

1.2.4.2 Andersen thermostat

The Andersen thermostat is a proposal in molecular dynamics simulation for keeping constant temperature conditions. It is based on the reassignment of a chosen atom or molecule's velocity. The new velocity is given by Maxwell–Boltzmann statistics for the given temperature²⁵.

1.2.4.3 Berendsen thermostat

In Berendsen thermostat, the system is weakly coupled to a heat bath with some temperature. The thermostat suppresses fluctuations of the kinetic energy of the system and

therefore cannot produce trajectories consistent with the canonical ensemble. The temperature of the system is corrected such that the deviation exponentially decays with some time constant²⁶.

1.3 Objective

In this study, the diffusion and adsorption of methane (CH_4) in ZIF-8 pore have been assessed, in order to understand methane behavior in ZIF-8 pore by using DFTB and DFTB/MD methods.



CHAPTER II

COMPUTATIONAL DETAILS

2.1 Molecular dynamics simulation

Full optimizations of ZIF-8 and CH₄ molecules were carried out using DFTB method. The optimized ZIF-8 unit cell length has been found by vary the unit cell length. Molecular dynamics simulation was used to simulate the systems that consist of ZIF-8 with 8, 12 and 16 CH₄ molecules. All calculations were performed with DFTB+ version 1.3 program²⁷.

2.2 Definitions of reaction terms

2.2.1 Diffusion of small gases in ZIF-8

2.2.1.1 The mean-square displacement (MSD)

The mean-square displacement (*MSD*)²⁸ is one of the most important dynamical quantities that can be calculated from the time evolution of a simulated system defined by,

$$MSD = \frac{1}{N} \left\langle \sum_{i=1}^N [r_i^c(t) - r_i^c(0)]^2 \right\rangle \quad (2.1)$$

where $r_i^c(t)$ is the location of the center of mass of particle i at time t .

2.2.1.2 The self-diffusion coefficient

The self-diffusion coefficient can be calculated from the long time limit of *MSD* using Einstein relation. It is a direct measurement of *MSD* of guest molecules under equilibrium conditions.

$$D_i = \frac{1}{6} \lim_{t \rightarrow \infty} \frac{d}{dt} \langle [r_i^c(t) - r_i^c(0)]^2 \rangle \quad (2.2)$$

2.2.1.3 The radial distribution function (RDF)

The radial distribution function (RDF) represents by $g(r)$. For a system of N atoms in a volume V (with number density ρ), RDF is defined by the expression.

$$\rho g(r) = \frac{1}{N} \langle \sum_{i=1}^N \sum_{j \neq i}^N \delta(r - r_{ij}) \rangle \quad (2.3)$$

where the bracket indicates time average and r_{ij} is the distance between atoms i and j . If we explicitly consider the time average over the total of M time steps, t_k , in the MD, we have

$$g(r) = \frac{\sum_{k=1}^M N_k(r, \Delta r)}{M \left(\frac{1}{2} N \right) \rho V(r, \Delta r)} \quad (2.4)$$

where $N(r, \Delta r)$ and $V(r, \Delta r)$ are the number of local atoms and volume between the spherical shells of radius r and $(r + \Delta r)$ with the shell centered on another atom.

2.2.2 Adsorption of small gases in ZIF-8

The adsorption energy (ΔE_{ads}) for gas molecules adsorbed on the beryllium oxide has been computed by the equation

$$\Delta E_{ads} = E_{G/ZIF8} - (E_G + E_{ZIF8}) \quad (2.5)$$

where $E_{G/ZIF8}$ is the total energy of gas adsorbed on ZIF-8, E_{ZIF8} is the total energy of isolated ZIF-8 and E_G is total energy of free gas molecule.



CHAPTER III

RESULTS AND DISCUSSIONS

ZIF-8 structure and diffusion of CH₄ in the ZIF-8 structure have been studied. Adsorption energies of CH₄ in the ZIF-8 structure and their thermodynamics properties have been obtained.

3.1 Geometry optimization of ZIF-8

The optimized structures of ZIF-8 obtained by the SCC-DFTB method with different conditions are shown in Figure 3.1 and the unit cell parameter $a = 16.705 \text{ \AA}$ at 298.15 K was found. The optimized a parameter was obtained by taking the minimum point of the quadratic equation of $E = ar^2 + br + c$ which is the curve fit as shown in Figure 3.2. The selected geometry parameters of the SCC-DFTB-optimized structures of the unit cell size of ZIF-8 are listed in Table 3.1. It shows that bond lengths and bond angles of SCC-DFTB-optimized unit cell size structure is closed to the B3LYP/6-311++g(2d,2p)-optimized structure of ZIF-8 component and in good agreement with the X-ray diffraction structure.²⁹

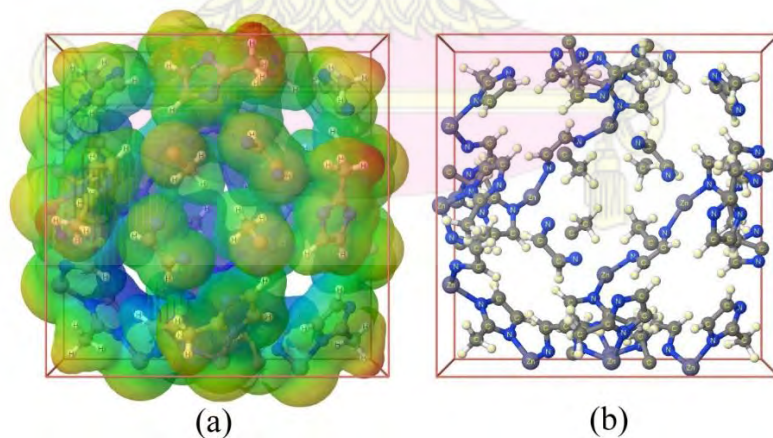


Figure 3.1 The SCC-DFTB optimized unit cell-sized ZIF-8 structure (a) with and (b) without electrostatic surfaces.

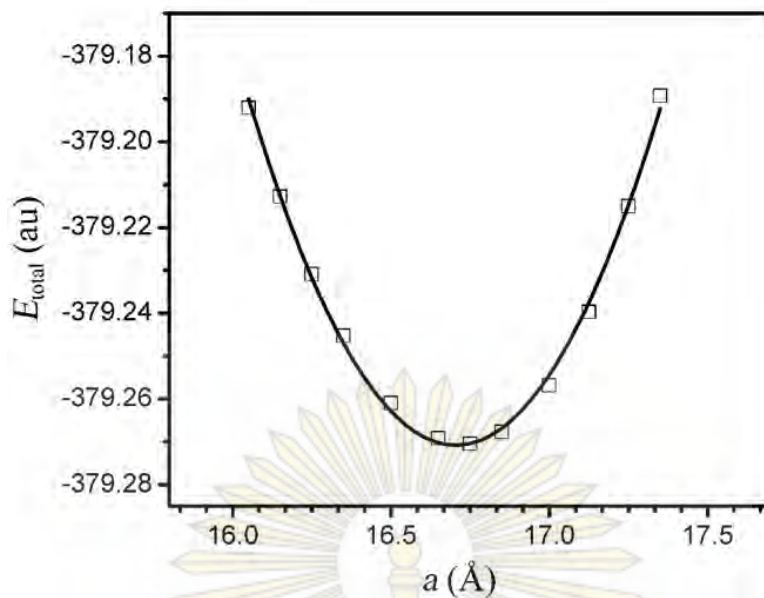


Figure 3.2 Plot of total energy (au) of the ZIF-8 against lattice parameter a including its quadratic function ($E_{\text{total}} = 0.18857a^2 - 6.30013a - 326.64929$). The minimum value derived by equation $dE_{\text{total}}/da = 0$, $a = 16.7050$ Å was obtained.

Table 3.1 Selected geometrical parameters of ZIF-8, based on X-ray diffraction and DFTB optimized structures.

Parameters ^a	X-ray ^b	Component ^c	Unit cell ^d
Bond length (Å)			
Zn1-N1	1.989	1.972	1.975
Zn1-N1'	1.989	1.973	1.975
Zn2-N2	1.989	–	1.975
C3-N1	1.340	1.362	1.356
C3-N2	1.340	1.354	1.356
C2-N2	1.379	1.378	1.377
C1-C2	1.360	1.394	1.387
C1-N1	1.379	1.375	1.377
C3-C4	1.494	1.486	1.482
C4-H1	1.026	1.106	1.103
C4-H2	1.030	1.098	1.097
Angle (°)			
C2-C1-N1	108.2	106.8	107.5
C1-N1-Zn1	126.9	126.3	124.6
C3-N1-Zn1	127.2	126.4	127.5
C1-N1-C3	105.8	107.3	107.8
N1-Zn1-N1'	109.4	109.4	109.8
N1-C3-N2	112.0	110.9	109.4
N1-C3-C4	124.0	123.7	125.3
C1-C2-N2	108.2	108.8	107.5
C2-N2-C3	105.8	106.1	107.8
Zn2-N2-C3	127.2	–	127.5
N2-C3-C4	124.0	125.4	125.3
C3-C4-H1	115.8	111.8	111.1
C3-C4-H2	111.1	110.4	110.7

^a The structure is defined in Figure 3.3.

^b Taken from ref. 29.

^c B3LYP/6-311++g(2d,2p)-optimized structure.

^d SCC-DFTB optimized unit cell-size structure.

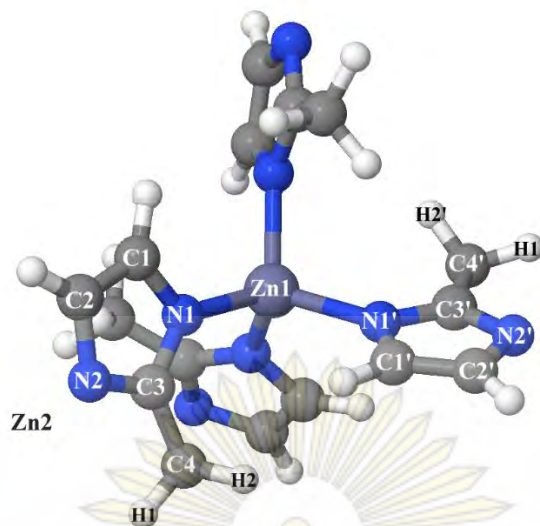


Figure 3.3 Labeling atoms of ZIF-8 for as referred in Table 3.1.

3.2 Energies of various structures of the ZIF-8 pore

Energies of SCC-DFTB-optimized structure and MD simulations of various situations of ZIF-8 pore are shown in Table 3.2. It shows the relative energies of ZIF-8 pore structures relative to the X-ray structure, based on the SCC-DFTB-optimized, Andersen and Berendsen thermostat/MD simulations are -323.58 , 107.32 and 148.11 kcal/mol, respectively. As the narrow temperature fluctuations of the Berendsen thermostat compared with the Andersen thermostat as shown in Figure 3.4, the MD simulation with Berendsen thermostat was therefore selected to be employed in this work. In Berendsen thermostat, the velocities of every particle are scaled by a time factor. Therefore, the kinetic energy gives the desired target temperature.³⁰ On the other hand, when using the Andersen thermostat a number of particles are randomly selected to be given a new velocities.³⁰ The systems, that we studied, are large systems. So, Berendsen thermostat is more suitable than Andersen thermostat.

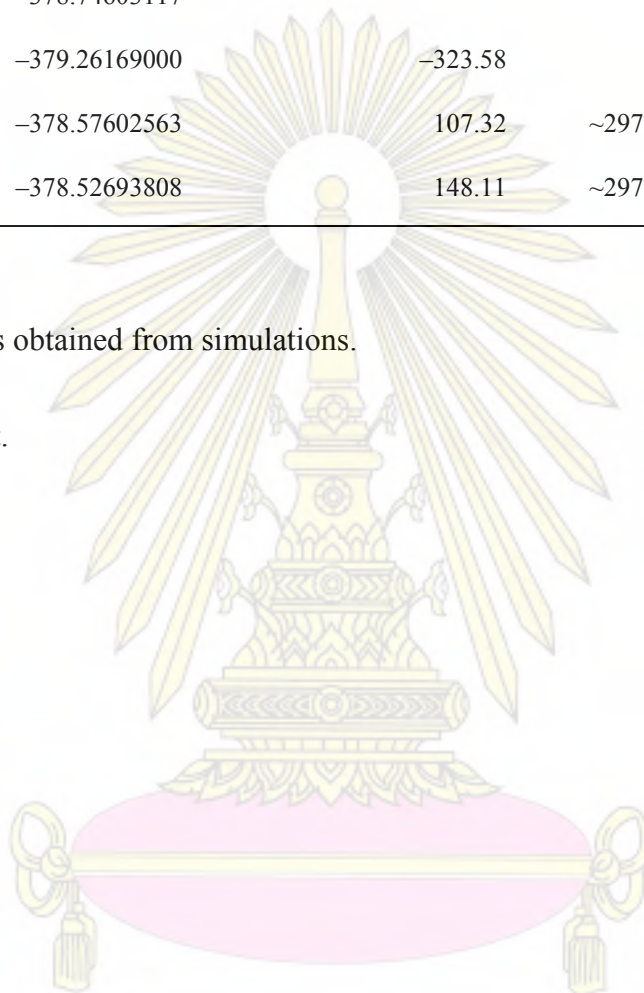
Table 3.2 Total energies of SCC–DFTB–optimized structure and MD simulations of various situations of ZIF–8 pore

ZIF–8	E_{total} , au	ΔE_{rel} , kcal mol ⁻¹	T , K
X–ray	-378.74603117	–	–
Optimized	-379.26169000	-323.58	298.15
A/MD sim ^a	-378.57602563	107.32	~297.28±0.17 ^b
B/MD sim ^c	-378.52693808	148.11	~297.74±0.05 ^b

^a Andersen thermostat.

^b Average temperatures obtained from simulations.

^c Berendsen thermostat.



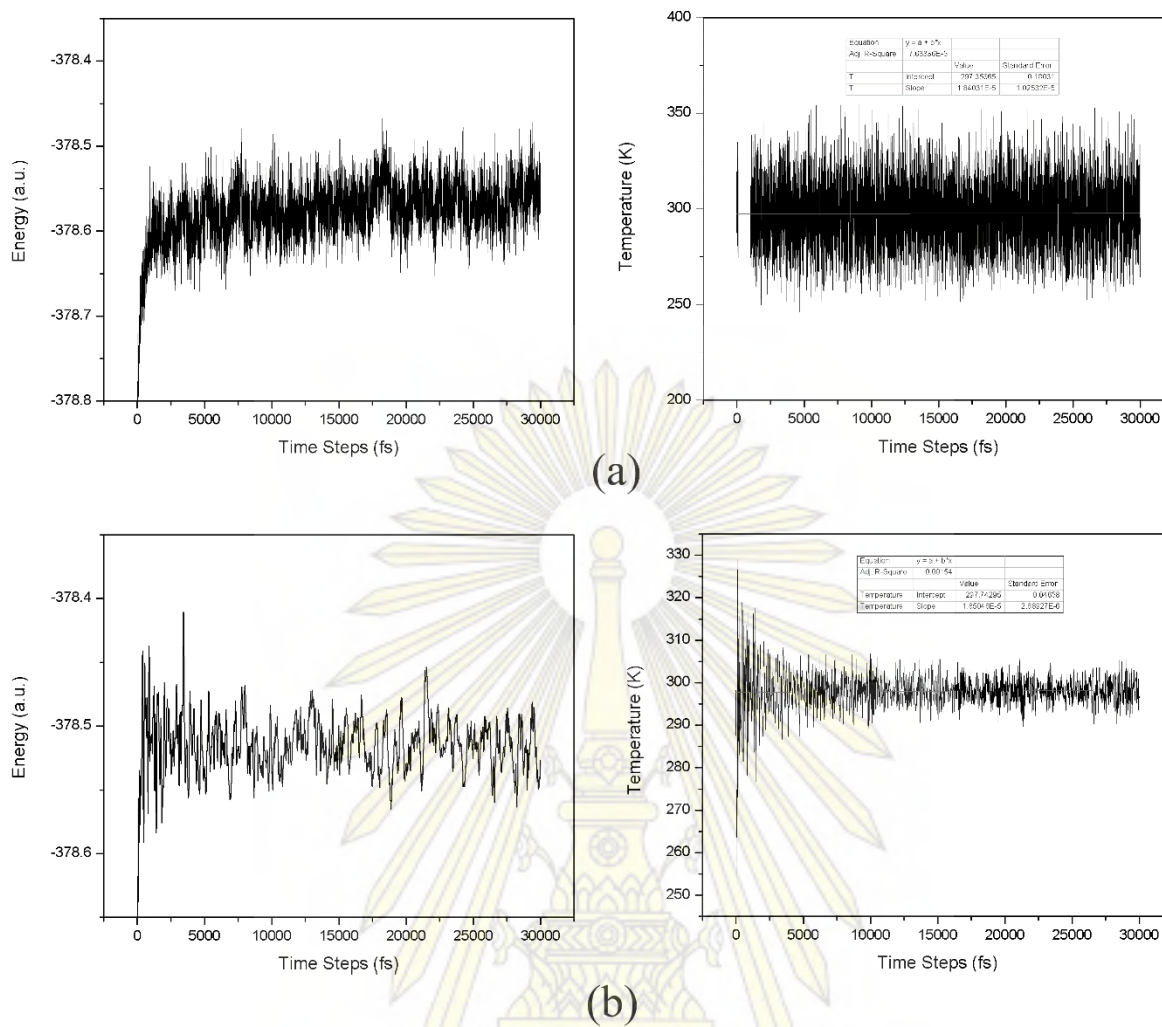


Figure 3.4 MD simulations based on (a) Andersen and (b) Berendsen thermostats, NVT ensemble presented as energies (left) and temperature (right) fluctuations of ZIF-8 with unit cell-sized structure.

3.3 MD simulations and dynamical quantities of CH₄ in ZIF-8 pore

The MD simulations based on the SCC-DFTB method with the Berendsen thermostat for the host-guest systems of 8, 12 and 16 molecules of methane gas in ZIF-8 pores were performed as shown in Table 3.3. The self-diffusion coefficient for 8, 12 and 16 CH₄ system are $1.61 \pm 0.08 \times 10^{-9}$, $1.92 \pm 0.05 \times 10^{-9}$ and $2.09 \pm 0.03 \times 10^{-9} \text{ m}^2\text{s}^{-1}$, respectively. These results show that the self-diffusion coefficient for the system of methane in ZIF-8 depends on the number of methane molecules in ZIF-8, the self-diffusion coefficient of the large number of methane molecules system is higher value than the small number of methane molecules system. As seen in Table 3.3 the adsorption energy of CH₄ on ZIF-8 for 8, 12 and 16 methane molecules is -3.86, -4.38 and -4.49 kcal/mol, respectively. These adsorption energies are not significantly different. Therefore, the adsorption affinity of those host-guest systems is not different.

Figure 3.5 represents the center-of-mass radial density profile of CH₄ from the center of the ZIF-8 unit-cell. These graphs show the mass distribution of molecules of methane from the host center. In 12 and 16 molecules of methane systems, the peaks are clearly separated, but in the 8 molecules of methane system, the peaks are not separated. Because this system has a low gas loading, the distribution of gas is not obviously observed. In addition, Table 3.3 shows values on maxima of density peaks of center-of-mass (CoM) based CH₄ from the ZIF-8 unit-cell center. These values combine with the center-of-mass radial density profile made. We understand to the distribution of molecules of methane from the ZIF-8 unit cell center. The molecules of methane spread from the center of host to 2 layers. The distances from the center to the first layer are ~ 3.1 , 2.9 and 2.8 Å for 8, 12 and 16 molecules, respectively. For the second layer, the distances are 5.1, 5.1 and 5.3 Å, respectively.

Next, Figure 3.6 shows the C–C radial distribution function of CH₄ molecules in the systems. As seen in Figure 3.6 strong RDF peaks between C atoms of methane appear at 3.90, 3.85 and 3.80 Å for 8, 12 and 16 molecules of methane system. The another peak in the graphs is a broad peak. This peak appears around 7 Å for all systems. For the 8 molecules system, this peak is not clearly observable but, for the 12 and 16 molecule systems, this peak is observable. On the other hand, the values of $g_{cc}(r)$ is 0 in the range of 0 - ~3 and over 10 Å from the carbon atom of methane molecules. Thus, we can approximate the distribution of methane molecules around the reference methane molecule that, the reference methane molecule is surrounded by 2 layers of methane molecules. The first layers are 3.90, 3.85 and 3.80 Å from the reference molecule for 8, 12 and 16 molecules systems, the second layer is around 7 Å for all system. In the short range distance (0 - ~3 Å) and too long range distance (over 10 Å), the molecules of methane will not appear in this region. In the larger system, the first layer distance is shorter than in the smaller systems because the number of guest molecule increased but the host has the constant volume. So, the molecules of methane in the larger number of molecules system have the closer packing than smaller systems. Two layers, the first and second can be depicted as shown in Figure 3.7. Figure 3.8 shows the C–C radial distribution function of CH₄ molecules in terms of ratio of number of methane molecules $n(r)$ and number of methane molecules $N(r)$. From these graphs we can calculate amount of the methane molecules that surround the reference molecule. From Table 3.3, the first layers have 2.77, 4.49 and 6.23 molecules of methane and the second layers have 4.23, 6.51 and 8.72 molecules of methane for 8, 12 and 16 guest molecules system, respectively. The CH₄ molecules for the first and second layers respectively separated 5.4, 5.4 and 5.5 Å for 8,12 and 16 molecules systems, see Figure 3.8.

Now, we know about the distribution of methane in ZIF-8. Thus, we can explain the relation between the self-diffusion coefficient and the numbers of molecule of methane. When the sorption sites are saturated with guest molecules in relatively high loadings, this can cause an increase in the diffusion with increasing loading. As seen as Figure 3.9 the self-diffusion coefficient is a function of the number of methane molecules. The equation is therefore written as $D_s = -4.375 \times 10^{-12} N^2 + 1.65 \times 10^{-10} N + 5.70 \times 10^{-10} \text{ m}^2\text{s}^{-1}$. Where D_s is the self-diffusion coefficient and N is the number of methane molecules. The values of self-diffusion coefficient obtained in this work are in good agreement with the results of Stallmach *et al.*³¹ and García-Sánchez *et al.*³². The above equation should accurately predict the self-diffusion coefficient at 298.15 K.



Table 3.3 The self-diffusion coefficients (D_s), structures and energetics of CH₄ in various molecular loading numbers in the ZIF-8 unit cell, at 298 K.

System	$D_s, \text{m}^2\text{s}^{-1}$	Rdf ^b			$R_{\text{CoM}}, \text{\AA}^{\text{c,d}}$	$\Delta E_{\text{ads}}^{\text{e}}, \text{kcal mol}^{-1}$
		$r_{\text{C-C}}, \text{\AA}^{\text{a}}$	1 st	2 nd		
8 CH ₄	$1.61 \pm 0.08 \times 10^{-9}$	3.90	2.77	4.23	~3.1, 5.1	-3.86
12 CH ₄	$1.92 \pm 0.05 \times 10^{-9}$	3.85	4.49	6.51	2.9, 5.1	-4.38
16 CH ₄	$2.09 \pm 0.03 \times 10^{-9}$	3.80	6.23	8.72	2.8, 5.3	-4.49

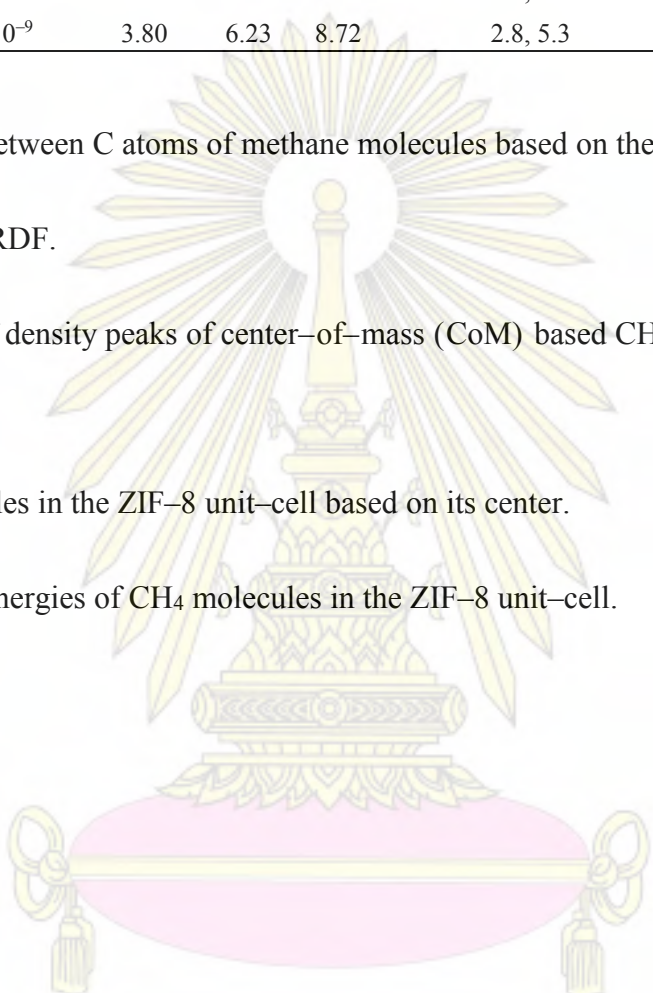
^a Mean displacement between C atoms of methane molecules based on the RDF.

^b Values based on the RDF.

^c Values on maxima of density peaks of center-of-mass (CoM) based CH₄ from the ZIF-8 unit-cell center.

^d Existing CH₄ molecules in the ZIF-8 unit-cell based on its center.

^e Average adsorption energies of CH₄ molecules in the ZIF-8 unit-cell.



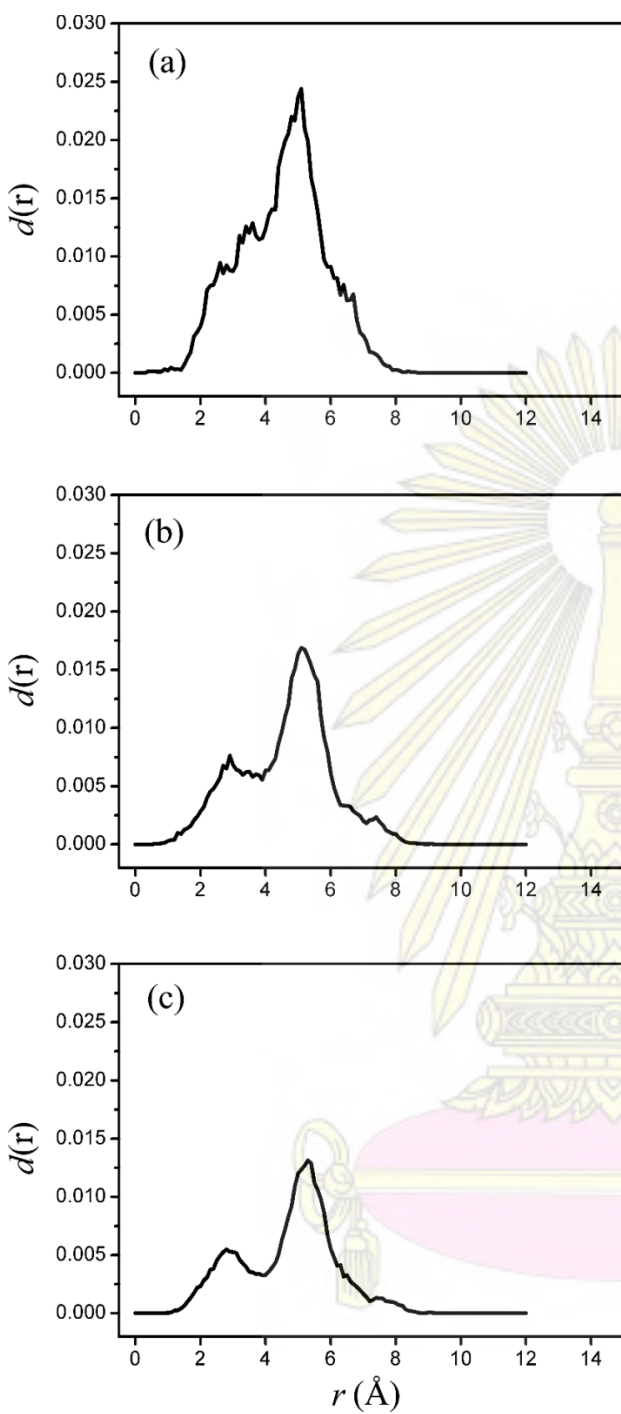


Figure 3.5 The center-of-mass radial density profile of CH₄ from the center of the ZIF-8 unit-cell pour for the systems containing (a) 8, (b) 12 and (c) 16 CH₄ molecules.

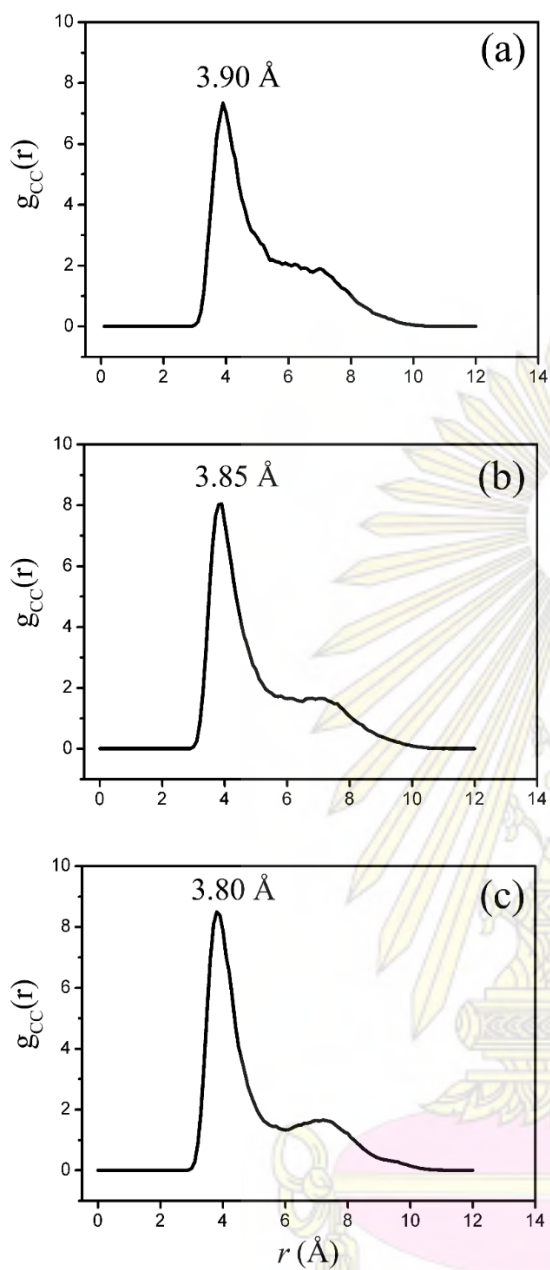


Figure 3.6 The C–C radial distribution function of CH₄ molecules in the systems of (a) 8, (b) 12 and 16 CH₄ molecules in the ZIF–8 unit cell.

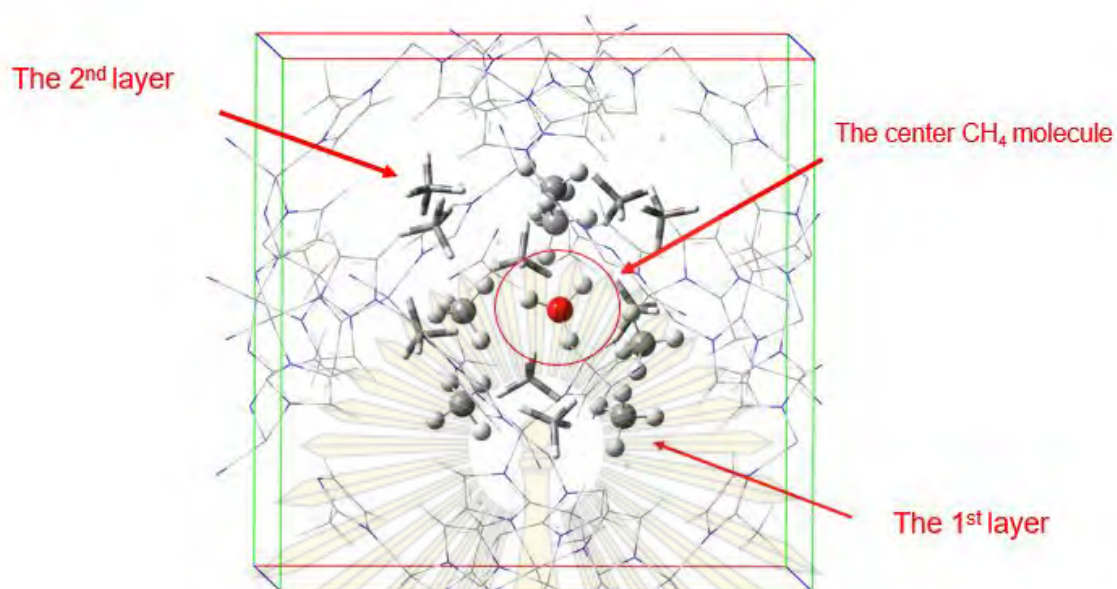


Figure 3.7 The final snapshot of the simulation box involves the distribution of methane 16 molecules.

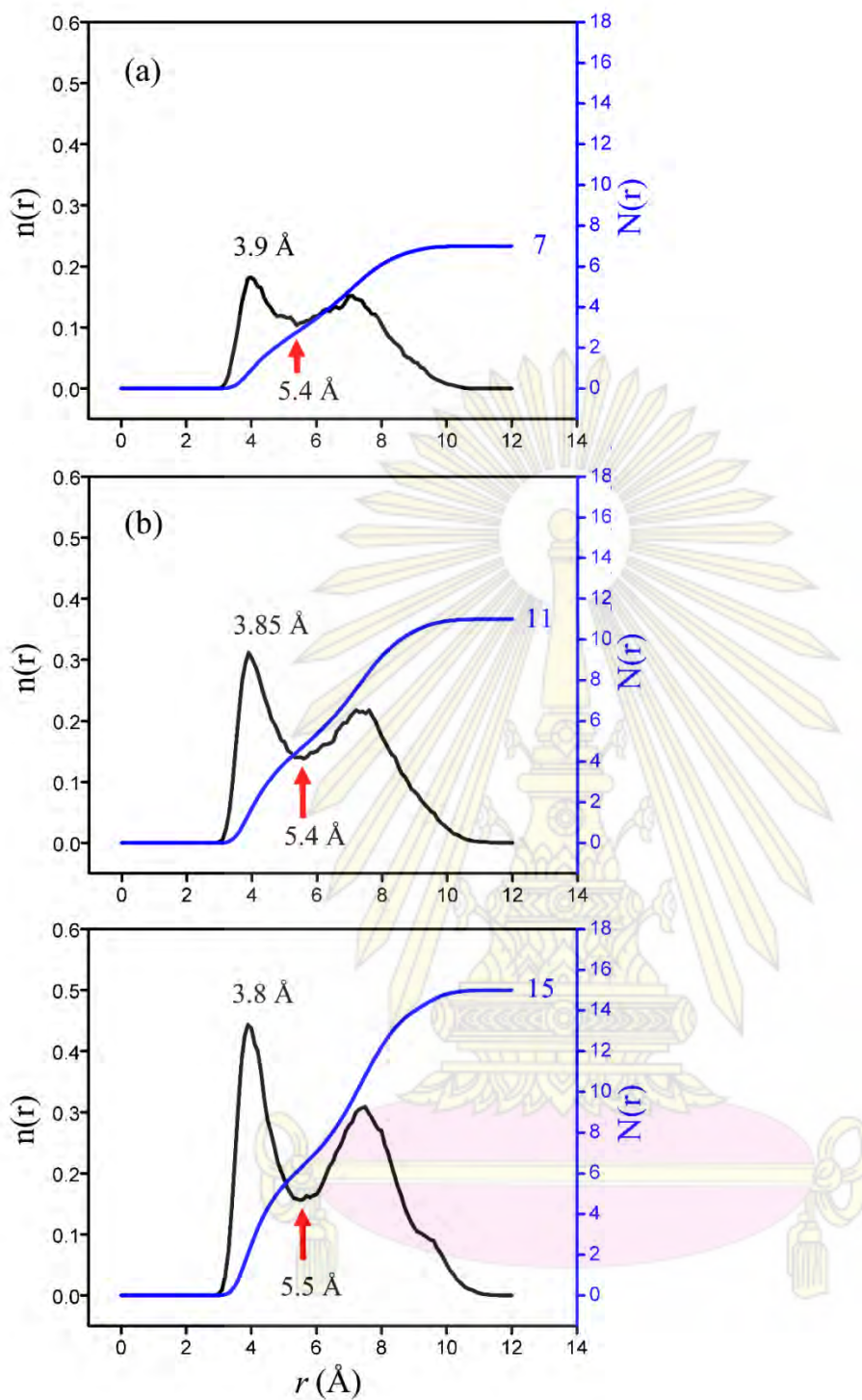


Figure 3.8 The C–C radial distribution function of CH_4 molecules in terms of $n(r)$ (left axis) and $N(r)$ (right axis) of (a) 8, (b) 12 and 16 CH_4 molecules in the ZIF–8 unit cell.

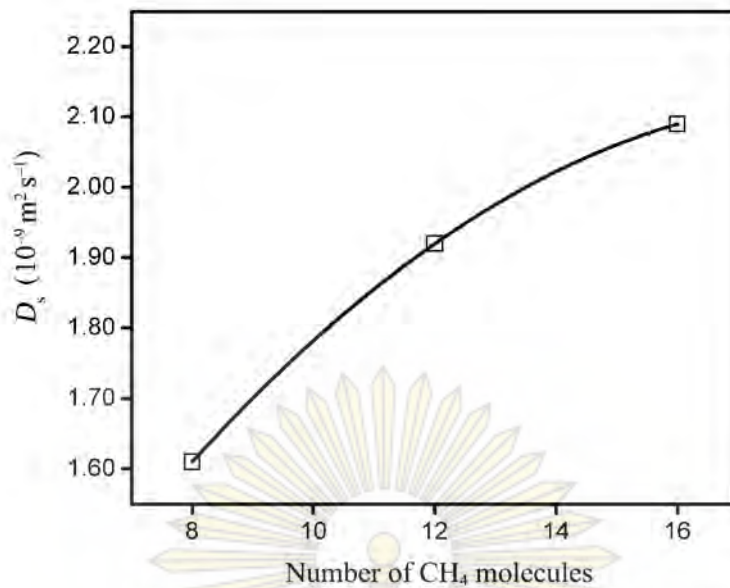


Figure 3.9 Plot of D_s against the number (N) of methane molecules in the ZIF-8 unit cell. The dot line is the quadratic fitted curve represented as $D_s = -4.375 \times 10^{-12} N^2 + 1.65 \times 10^{-10} N + 5.70 \times 10^{-10}$.

CHAPTER IV

CONCLUSIONS

The ZIF-8 structure was optimized by SCC-DFTB. The bond lengths and bond angles of the optimized structure in good agreement with the X-ray diffraction structure. The adsorption and diffusion of 8, 12 and 16 molecules of methane in ZIF-8 pore have been studied by SCC-DFTB/MD method with Berendsen thermostat. The self-diffusion coefficient of the systems is related to the number of methane molecules as $D_s = -4.375 \times 10^{-12} N^2 + 1.65 \times 10^{-10} N + 5.70 \times 10^{-10}$. From the center of ZIF-8 unit cell, the methane molecules distribute to 2 layers. Distances from the center of host is ~ 3 and ~ 5 Å for the first and second layers, respectively. The C–C radial distribution function of CH₄ molecules shows the distribution of methane molecules. The reference methane molecule is surround by others methane molecules. The methane molecules spread in two layers, the first layers have 3.90, 3.85 and 3.80 Å from the reference molecule for all systems. The first layer distances decreased when the number of methane molecules in the system increased because the host has the constant volume while the number of guest molecules increased and the second layer is around 7 Å for all systems. The adsorption energies for all systems are not significantly different. Thus, the adsorption energy does not depend on gas loading.

REFERENCES

1. Park, K. S.; Ni, Z.; Côté, A. P.; Choi, J. Y.; Huang, R.; Uribe-Romo, F. J.; Chae, H. K.; O'Keeffe, M.; Yaghi, O. M., Exceptional chemical and thermal stability of zeolitic imidazolate frameworks. *Proceedings of the National Academy of Sciences* **2006**, *103* (27), 10186-10191.
2. Springuel-Huet, M.-A.; Nossov, A.; Guenneau, F.; Gedeon, A., Flexibility of ZIF-8 materials studied using ¹²⁹Xe NMR. *Chemical Communications* **2013**, *49* (67), 7403-7405.
3. Fairen-Jimenez, D.; Moggach, S. A.; Wharmby, M. T.; Wright, P. A.; Parsons, S.; Düren, T., Opening the Gate: Framework Flexibility in ZIF-8 Explored by Experiments and Simulations. *Journal of the American Chemical Society* **2011**, *133* (23), 8900-8902.
4. Zhou, K.; Mousavi, B.; Luo, Z.; Phatanasri, S.; Chaemchuen, S.; Verpoort, F., Characterization and properties of Zn/Co zeolitic imidazolate frameworks vs. ZIF-8 and ZIF-67. *Journal of Materials Chemistry A* **2017**, *5* (3), 952-957.
5. Pimentel, B. R.; Lively, R. P., Enabling Kinetic Light Hydrocarbon Separation via Crystal Size Engineering of ZIF-8. *Industrial & Engineering Chemistry Research* **2016**, *55* (48), 12467-12476.
6. García Blanco, A. A.; Vallone, A. F.; Korili, S. A.; Gil, A.; Sapag, K., A comparative study of several microporous materials to store methane by adsorption. *Microporous and Mesoporous Materials* **2016**, *224*, 323-331.
7. Lai, L. S.; Yeong, Y. F.; Chew, T. L.; Lau, K. K.; Azmi, M. S., CO₂ and CH₄ gas permeation study via zeolitic imidazolate framework (ZIF)-8 membrane. *Journal of Natural Gas Science and Engineering* **2016**, *34*, 509-519.

8. Haranczyk, M.; Lin, L.-C.; Lee, K.; Martin, R. L.; Neaton, J. B.; Smit, B., Methane storage capabilities of diamond analogues. *Physical Chemistry Chemical Physics* **2013**, *15* (48), 20937-20942.
9. Wu, X.; Huang, J.; Cai, W.; Jaroniec, M., Force field for ZIF-8 flexible frameworks: atomistic simulation of adsorption, diffusion of pure gases as CH₄, H₂, CO₂ and N₂. *RSC Advances* **2014**, *4* (32), 16503-16511.
10. Krokidas, P.; Castier, M.; Moncho, S.; Brothers, E.; Economou, I. G., Molecular Simulation Studies of the Diffusion of Methane, Ethane, Propane, and Propylene in ZIF-8. *The Journal of Physical Chemistry C* **2015**, *119* (48), 27028-27037.
11. Eyer, S.; Stadie, N. P.; Borgschulte, A.; Emmenegger, L.; Mohn, J., Methane preconcentration by adsorption: a methodology for materials and conditions selection. *Adsorption* **2014**, *20* (5), 657-666.
12. Alirezaie, A. H. H.; Navarchian, A. H.; Sabzyan, H., Molecular dynamics simulation of gas diffusion in polyethylene-clay nanocomposites with different silicate layers configurations. *Polymer Science Series A* **2016**, *58* (3), 487-498.
13. Kadoura, A.; Narayanan Nair, A. K.; Sun, S., Molecular Dynamics Simulations of Carbon Dioxide, Methane, and Their Mixture in Montmorillonite Clay Hydrates. *The Journal of Physical Chemistry C* **2016**, *120* (23), 12517-12529.
14. Fairen-Jimenez, D.; Galvelis, R.; Torrisi, A.; Gellan, A. D.; Wharmby, M. T.; Wright, P. A.; Mellot-Draznieks, C.; Duren, T., Flexibility and swing effect on the adsorption of energy-related gases on ZIF-8: combined experimental and simulation study. *Dalton Transactions* **2012**, *41* (35), 10752-10762.

15. Koskinen, P.; Mäkinen, V., Density-functional tight-binding for beginners. *Computational Materials Science* **2009**, *47* (1), 237-253.
16. Garberoglio, G.; Taioli, S., Modeling flexibility in metal–organic frameworks: Comparison between Density-Functional Tight-Binding and Universal Force Field approaches for bonded interactions. *Microporous and Mesoporous Materials* **2012**, *163*, 215-220.
17. Levine, I. N., *Quantum Chemistry 6Th Ed.* Prentice-Hall Of India Pvt. Limited: 2009.
18. Young, D., *Computational Chemistry: A Practical Guide for Applying Techniques to Real World Problems.* Wiley: 2004.
19. Elstner, M.; Seifert, G., Density functional tight binding. *Philosophical Transactions of the Royal Society A: Mathematical, Physical and Engineering Sciences* **2014**, *372* (2011).
20. Oliveira, A. F.; Seifert, G.; Heine, T.; Duarte, H. A., Density-functional based tight-binding: an approximate DFT method. *Journal of the Brazilian Chemical Society* **2009**, *20*, 1193-1205.
21. Petrenko, R.; Meller, J., Molecular Dynamics. In *eLS*, John Wiley & Sons, Ltd: 2001.
22. Zhou, Y.; Wang, S.; Li, Y.; Zhang, Y., Chapter Five - Born–Oppenheimer Ab Initio QM/MM Molecular Dynamics Simulations of Enzyme Reactions. In *Methods in Enzymology*, Gregory, A. V., Ed. Academic Press: 2016; Vol. Volume 577, pp 105-118.
23. Groenhof, G., Introduction to QM/MM Simulations. In *Biomolecular Simulations: Methods and Protocols*, Monticelli, L.; Salonen, E., Eds. Humana Press: Totowa, NJ, 2013; pp 43-66.
24. Gibbs, J. W., *Elementary Principles in Statistical Mechanics.* Dover Publications: 2014.
25. Andersen, H. C., Molecular dynamics simulations at constant pressure and/or temperature. *The Journal of Chemical Physics* **1980**, *72* (4), 2384-2393.

26. Berendsen, H. J. C.; Postma, J. P. M.; Gunsteren, W. F. v.; DiNola, A.; Haak, J. R., Molecular dynamics with coupling to an external bath. *The Journal of Chemical Physics* **1984**, *81* (8), 3684-3690.
27. Aradi, B.; Hourahine, B.; Frauenheim, T., DFTB+, a Sparse Matrix-Based Implementation of the DFTB Method. *The Journal of Physical Chemistry A* **2007**, *111* (26), 5678-5684.
28. Kowsari, M. H.; Naderlou, S., Understanding the dynamics, self-diffusion, and microscopic structure of hydrogen inside the nanoporous Li-LSX zeolite. *Microporous and Mesoporous Materials* **2017**, *240*, 39-49.
29. Novaković, S. B.; Bogdanović, G. A.; Heering, C.; Makhloufi, G.; Francuski, D.; Janiak, C., Charge- Density Distribution and Electrostatic Flexibility of ZIF- 8 Based on High-Resolution X-ray Diffraction Data and Periodic Calculations. *Inorganic Chemistry* **2015**, *54* (6), 2660-2670.
30. Julin, J.; Napari, I.; Vehkamäki, H., Comparative study on methodology in molecular dynamics simulation of nucleation. *The Journal of Chemical Physics* **2007**, *126* (22), 224517.
31. Stallmach, F.; Pusch, A.-K.; Splith, T.; Horch, C.; Merker, S., NMR relaxation and diffusion studies of methane and carbon dioxide in nanoporous ZIF-8 and ZSM-58. *Microporous and Mesoporous Materials* **2015**, *205*, 36-39.
32. García-Sánchez, A.; Dubbeldam, D.; Calero, S., Modeling Adsorption and Self-Diffusion of Methane in LTA Zeolites: The Influence of Framework Flexibility. *The Journal of Physical Chemistry C* **2010**, *114* (35), 15068-15074.

VITAE

My name is Nontawat Ploysongsri. I was born on 24th February, 1995. My address is 38 Village No. 1, Dontan Sub-district, Muang Suphanburi district, Suphanburi 72000. My contact is 0882989010 and nonchem4670@gmail.com. I studied primary school at Anuban Suphanburi School during 1999-2006, high school at Kanchanapisek Wittayalai Suphanburi School during 2007-2012 and Bachelor's degree of Science at Chulalongkorn University during 2013-2016.

